International Journal of Difference Equations (IJDE).
ISSN 0973-6069 Volume 17, Number 2 (2022), pp. 347-360

https://www.ripublication.com/ijde.htm

Corona Virus Impact on Bifurcated Artery Using Micropolar Fluid Model

G. Madhava Rao[*1], D. Srinivasacharya[2], G Venkata Suman[3] and V. Dhanunjana Chari[4]

[1]*Department of Mathematics, Mallareddy University, Hyderabad, Telangana, India.*

[2]*Department of Mathematics, National Institute of Technology, Warangal, Telangana, India.*
[3]*Department of Mathematics, Mallareddy University, Hyderabad, Telangana, India.*

[4]*Department of Physics, Mallareddy University, Hyderabad, Telangana, India.*

Abstract

This article deals with pulsatile nature of blood flow in Corona virus affected person Carotid bifurcated artery with mild stenosis in the parent lumen by considering blood as micropolar fluid. When a person exposed with Corona virus, there is a possibility of plaque formation in the carotid bifurcated artery due to high usage of antibiotics. The arterial forming of division in Carotid is presumed to be a straight cylinder of restricted length and is symmetric about its axis. Mathematically the geometry of branched artery is changed to a rectangular shape with the radial coordinate transformations. Physical quantities such as shear stress, flow rate and impedance with respect to bifurcation angle, pulsatile nature are numerically computed on both sides of the apex and their significances are illustrated through graphs.

Keywords: Corona Virus, Carotid Bifurcated artery; Micropolar fluid, Pulsatile flow; Womersley number.

MSC 2010 No.: 76A05, 74S20

1. Introduction

Corona virus (COVID-19) disease was initially described in Wuhan labs, China, in patients complaining of flu like symptoms. With in the short span of time, it spread

more than 186 countries. COVID-19 is responsible for a great number of unwanted diseases and deaths everyday worldwide. The investigation of fluid dynamical characteristics of blood flow in Carotid bifurcated artery with mild construction due to COVID-19 has been attracted by many researchers. In the Covid-19 scenario, most of the doctors are using steroids like remdesivir to control the virus. Due to this, there is a possibility of deposition of obese material inside the walls of Carotid artery, is medically termed as stenosis. Once stenosis is formed and artery is bifurcated, the fluid mechanical, bio-mechanical and bio-chemical effects associated with the blood flow phenomenon are significantly changed.

Recent days extensive experimental and theoretical investigations have been carrying out on the control of Corona virus and subsequent side effects. Sapna Ratan Shah et.al. (2021)reported that COVID-19 patients with more impedance to blood flow are having high blood pressure and more chances to get heart stoke. Blood Flow Modeling in Coronary Arteries has been reviewed byVioleta Carvalho et.al.(2021)described a mathematical model to demonstrate the current status of the corona virus disease in Wuhan, China. Wu et.al. mentioned that zinc and hydroxychloroquine can control corona virus spread in the huma body.

Micropolar fluid model is initially introduced by Eringen (1966). Micropolar fluid exhibits the local rotary inertia efffects along with couple stresses. Micropolar fluids have several applications in engineering and physiological problems and rheologically describe human blood and polymeric suspensions. Mekheimer and Kot (2008) treated blood as micropolar fluid over a tapered artery having mild constriction in it. Shit and Roy (2011) analyzed flow of micropolar fluid over a constricted artery in existence of magnetic field, body acceleration and the pulsatile pressure gradient. Tthe unsteady nature of micropolar blood flow through irregularly constricted arteries with heat transfer characteristics has been studied by Saifuddin *et.al.* (2013). Heat and mass transfer of blood flow as micropolar fluid over a tapered constricted artery of permeable walls has been investigated by Ellahi *et.al.* (2014).

Several researchers have enticed in the study of blood flow in branched artery. Chakravarty and Sen (2006) explored the mathematical model for dynamic response of heat and mass transfer and convective diffusion process in blood flow over branched arteries in constricted condition. The influence of bifurcated angle, time on shear stress in femoral and coronary artery at the division of artery has been reported by Shaw et.al.(2009). Antonova *et.at.* (2012) explained the hemodynamical properties of blood flow and details of numerical simulations in the carotid artery bifurcation with stenosis. Bose and Benerji (2015) studied the magnetic particle behaviour on Newtonian bio-magnetic fluid flow in an aortic branched artery with a constriction. Srinivasacharya & Madhava Rao (2016) examined the impact of magnetic field and pulsatile pressure gradient on the flow of micropolar fluid through a bifurcated artery. Srinivasacharya & Madhava Rao (2018) analyzed the effects of couple stresses on pulsatile nature of blood flow over a branched artery with constriction. The influence of both post stenotic dilatation and stenosis has been analyzed by Bhuvana et.al. (2016).

In this paper, the impact of mild stenosis due to corona virus on bifurcated artery with mild stenosis in the parent lumen has been studied by considering blood as micropolar fluid.

2. Formulation of the problem

Consider Corona affected patient blood flow as laminar, unsteady, incompressible flow of micropolar fluid (which is modelled as blood) passing through carotid bifurcated constricted artery. The existence of flow segregation zones (if available) be eradicated by introducing deflection at the start of lateral junction and offset of junction. Consider cylindrical co-ordinate system such that 'r', 'θ' and 'z' are taken along radial, circumferential and axis of the artery directions respectively. Geometry of carotid branched artery is given in Fig.1. Flow is assumed to be axisymmetric, constriction is mild and Reynolds number is very small, so radial velocity can be neglected. With above mentioned assumptions, governing equations for the flow are

$$\frac{\partial p}{\partial r} = 0 \tag{1}$$

$$\rho \frac{\partial w}{\partial t} = -\frac{\partial p}{\partial z} + \frac{\kappa}{r}\frac{\partial}{\partial r}(r\nu) + (\mu + \kappa)\frac{1}{r}\frac{\partial}{\partial r}\left(r\frac{\partial w}{\partial r}\right) \tag{2}$$

$$\rho j \frac{\partial \nu}{\partial t} = -2\kappa\nu - \kappa\frac{\partial w}{\partial r} + \gamma\frac{\partial}{\partial r}\left(\frac{1}{r}\frac{\partial}{\partial r}(r\nu)\right) \tag{3}$$

Where w is axial velocity components, ν is component of microrotation vector, ρ, t and j are the fluid pressure, thickness, time variable and microgyration parameter respectively. μ, κ and γ are the dynamic viscosity, microrotation and spin gradient viscosities, respectively and fulfil the inequalities

$$\kappa \geq 0, 2\mu + \kappa \geq 0, 3\alpha_1 + \beta_1 + \gamma \geq 0, \gamma \geq |\beta| \tag{4}$$

The mathematical representation for the walls outside and inside to the artery with slight constriction in its parent artery are given by

$$R_1(z) = \begin{cases} a\,a_1(t), & 0 \leq z \leq d' \quad and \quad d' + l_0 \leq z \leq z_1 \\ \left(a - \dfrac{4\tau_m}{l_0^2}(l_0(z-d') - (z-d')^2\right)a_1(t), & d' \leq z \leq d' + l_0 \\ (a + r_0 - \sqrt{r_0^2 - (z-z_1)^2})a_1(t), & z_1 \leq z \leq z_2 \\ (2r_1 sec\beta + (z-z_2)tan\beta)a_1(t), & z_2 \leq z \leq z_{max} \end{cases} \tag{5}$$

$$R_2(z) = \begin{cases} 0, & 0 \leq z \leq z_3 \\ \left(\sqrt{(r_0')^2 - (z - z_3 - r_0')^2}\right)b_1(t), & z_3 \leq z \leq z_3 + r_0'(1 - sin\beta) \\ (r_0' cos\beta + z_4)\,b_1(t), & z_3 + r_0'(1 - sin\beta) \leq z \leq z_{max} \end{cases} \tag{6}$$

where a and r_1 are the radii of the main artery at non-constricted position and the daughter artery, r_0, r_0' represents radii of curvatures at start of lateral junction and division of branched artery, l_0 is length of mild constriction in parent artery, z_1 and z_2 represent locations of start of onset and offset of lateral junction, z_3 represent apex, τ_m is height of the constriction at $z = d' + l_0/2$, β is 50% of bifurcation angle and $z_{\max}$ is the finite length of the artery under and $a_1(t)$, $b_1(t)$ are given by

$$\left.\begin{aligned} a_1(t) &= 1-(\cos\omega t-1)k\exp(-k\omega t)\\ b_1(t) &= \frac{1}{a_1(t)} \end{aligned}\right\} \tag{7}$$

The curvature of radii r_0 and r'_0 are given by

$$r_0 = \frac{a-2r_1 sec\beta}{cos\beta-1} \quad \text{and} \quad r_0^{1} = \frac{(z_3-z_2)sin\beta}{1-sin\beta}$$

Where $z_2 = z_1 + r_0 \sin\beta$, $z_3 = z_2 + q_1$ and $z_4 = (z_3 - r_0'(1-\sin\beta))\tan\beta$.

Here $q \ll 1$defined for compatibility of the geometry which is a small number such that $0.1 \le q_1 \le 0.5$.

The pressure gradient of the pulsatile nature is assumed as

$$-\frac{\partial p}{\partial z} = G_0 + G_1\cos(\omega t) \tag{8}$$

where G_0 and G_1 are the amplitudes of pressure gradient and pulsatile component respectively and $\omega = 2\pi f_p$, f_p is pulsatile flow frequency.

The dimensionless scheme is given by

$$\left.\begin{aligned} &r = a\tilde{r}, w = w_0 w, p = \frac{Lw_0\mu p}{a^2}, z = L\ \tilde{z}, \nu = \frac{w_0\nu}{a}, j = a^2 j, d = L\ d,\\ &R_1(z) = a\ R_1(\tilde{z}), R_2(z) = a\ R_2(\tilde{z}), r_1 = a\ r_1, z_1 = a\ z_1, t = \frac{\tilde{t}}{\omega}\\ &a_1(\frac{t}{\omega}) = a_1, b_1(\frac{t}{\omega}) = b_1. \end{aligned}\right\} \tag{9}$$

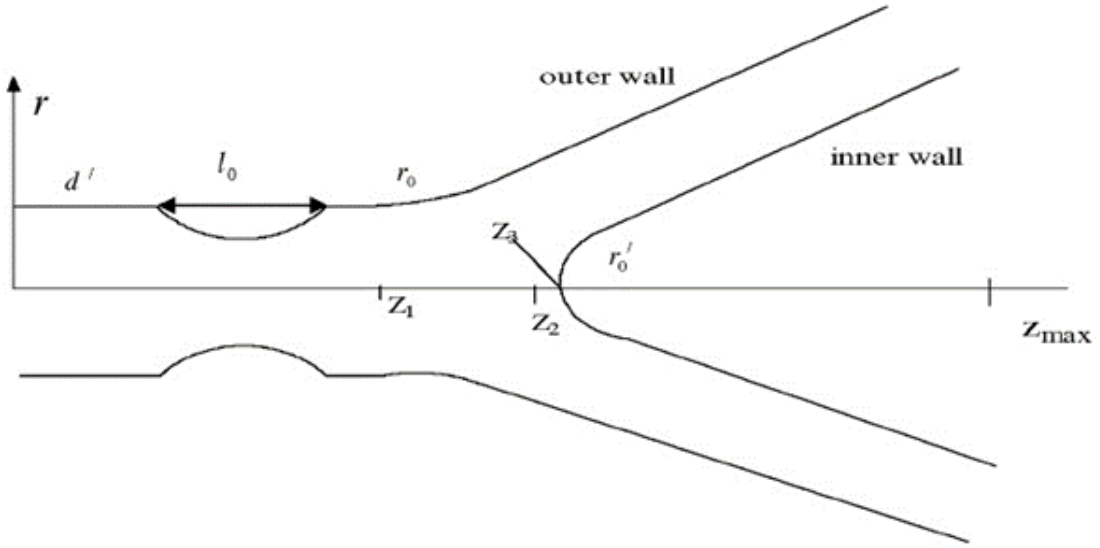

Figure 1: Geometry of the Carotid artery with Stenosis and Bifurcation.

where L and w_0 are the characteristic length and velocity, respectively.

Substituting (9) into the equations (1)-(7) and dropping the tildes, we have

$$R_w^2 \frac{\partial w}{\partial t} = -\frac{\partial p}{\partial z} + \left(\frac{N}{1-N}\right)\frac{1}{r}\frac{\partial}{\partial r}(r\nu) + \left(\frac{1}{1-N}\right)\frac{1}{r}\frac{\partial}{\partial r}\left(r\frac{\partial w}{\partial r}\right) \tag{10}$$

$$R_w^2 j\left(\frac{1-N}{N}\right)\frac{\partial \nu}{\partial t} = -2\nu - \frac{\partial w}{\partial r} + \left(\frac{2-N}{m^2}\right)\frac{\partial}{\partial r}\left(\frac{1}{r}\frac{\partial}{\partial r}(r\nu)\right) \tag{11}$$

$$R_1(z) = \begin{cases} a_1(t), & 0 \le z \le d' \quad and \quad d'+l_0 \le z \le z_1 \\ \left(1-\frac{4\tau_m}{l_0^2}(l_0(z-d')-(z-d')^2\right)a_1(t), & d' \le z \le d'+l_0 \\ (1+r_0-\sqrt{r_0^2-(z-z_1)^2})a_1(t), & z_1 \le z \le z_2 \\ (2r_1 sec\beta + (z-z_2)tan\beta)a_1(t), & z_2 \le z \le z_{max} \end{cases} \tag{12}$$

$$R_2(z) = \begin{cases} 0, & 0 \le z \le z_3 \\ \left(\sqrt{(r_0')^2-(z-z_3-r_0')^2}\right)b_1, & z_3 \le z \le z_3 + r_0'(1-sin\beta) \\ (r_0' cos\beta + z_4)b_1, & z_3 + r_0'(1-sin\beta) \le z \le z_{max} \end{cases} \tag{13}$$

$$\text{And } a_1 = 1-(\cos t - 1)k\exp(-kt), \quad b_1 = \frac{1}{a_1}, r_0 = \frac{1-2r_1 sec\beta}{cos\beta - 1} \text{ and } r_0' = \frac{(z_3-z_2)sin\beta}{1-sin\beta} \tag{14}$$

where $R_w^2 = \frac{a^2\rho\omega}{\mu}$-Womersley number, $N = \frac{\kappa}{\mu+\kappa}$-micropolar coupling number $(0 \le N \le 1)$ and $m^2 = \frac{a^2\kappa(2\mu+\kappa)}{\gamma(\mu+\kappa)}$-micropolar parameter.

The system of equations (10) and (11) reduced to a trditional Newtonian fluid model, when $N \to 0$ and $m \to \infty$.

Boundary conditions for physical problem in dimensionless form are

$$\left.\begin{array}{l} \frac{\partial w}{\partial r} = 0, \nu = 0, \text{on } r = 0 \text{ for } 0 \le z \le z_3, t > 0 \\ w = 0, \nu = 0 \text{ on } r = R_1(z,t) \text{ for all } z, t > 0 \\ w = 0, \nu = 0 \text{ on } r = R_2(z,t) \text{ for } z_3 \le z \le z_{max}, t > 0 \\ w = w_0, \nu = 0 \ at\ t = 0. \end{array}\right\} \tag{15}$$

As boundary of branched mild constricted artery is not in proper shape, it is transformed to proper shaped boundary using the following coordinate conversion

$$\xi = \frac{r-R_2}{R}, \text{ wherein R(z) = } R_1(z) - R_2(z) \tag{16}$$

Using (16) in (10) and (11) we get

$$\left(\frac{1-N}{N}\right)R_w^2 j\frac{\partial \nu}{\partial t} = -\frac{1}{R}\frac{\partial w}{\partial \xi} + \frac{(2-N)}{m^2R^2}\frac{\partial^2 \nu}{\partial \xi^2} - \left(2 + \frac{(2-N)}{m^2(\xi R + R_2)^2}\right)\nu$$
$$+ \frac{(2-N)}{m^2R(\xi R + R_2)}\frac{\partial \nu}{\partial \xi} + \left(\frac{1-N}{N}\right)R_w^2\frac{1}{R}\frac{\partial \nu}{\partial \xi}\left(\xi\frac{\partial R}{\partial t} + \frac{\partial R_2}{\partial t}\right) \tag{17}$$

$$(\frac{1-N}{N})R_w^2 j\frac{\partial \nu}{\partial t} = -\frac{1}{R}\frac{\partial w}{\partial \xi} + \frac{(2-N)}{m^2R^2}\frac{\partial^2 \nu}{\partial \xi^2} - \left(2 + \frac{(2-N)}{m^2(\xi R + R_2)^2}\right)\nu$$
$$+\frac{(2-N)}{m^2R(\xi R + R_2)}\frac{\partial \nu}{\partial \xi} + (\frac{1-N}{N})R_w^2\frac{1}{R}\frac{\partial \nu}{\partial \xi}(\xi\frac{\partial R}{\partial t} + \frac{\partial R_2}{\partial t}) \quad (18)$$

The boundary conditions (15) are transformed to the form

$$\frac{\partial w}{\partial \xi} = 0, \nu = 0, \text{on } \xi = 0 \text{ for } 0 \le z \le z_3$$
$$w = 0, \nu = 0 \text{ on } \xi = 1 \text{ for all } z \quad (19)$$
$$w = 0, \nu = 0 \text{ on } \xi = 0 \text{ for } z_3 \le z \le z_{max}$$
$$w = w_0, \nu = 0 \ \ at\ t = 0.$$

Solving the equations (18) and (19), we obtain the velocity and microrotation components.

The physical measures to be analyzed are the impedance, volume of flow and shear stress for both the arteries.

Impedance (resistance to flow) in daughter artery λ_d and in parent artery λ_p are calculated by using

$$\lambda_p = \left|\frac{z_3\frac{dp}{dz}}{Q_p}\right| for\ z < z_3\ and\ \lambda_d = \left|\frac{(z_{max} - z_3)\frac{dp}{dz}}{Q_d}\right| for\ z \ge z_3 \quad (20)$$

Flow rate in parent and artery daughter artery are determined using

$$Q_d = 2\pi R\left[R\int_0^1 \xi w d\xi + R_2\int_0^1 w d\xi\right] and\ Q_d = \pi R\left[R\int_0^1 \xi w d\xi + R_2\int_0^1 w d\xi\right]\Bigg\} \quad (21)$$

The wall shearing stress at both the walls of artery is given by

$$\tau_{ij} = \frac{1}{R}\frac{\partial w}{\partial \xi} + \frac{1}{4R\alpha^2(\xi R + R_2)^2}\frac{\partial w}{\partial \xi} - \frac{1}{4\alpha^2R^3}\frac{\partial}{\partial \xi}\left(\frac{\partial^2 w}{\partial \xi^2}\right) - \frac{1}{4R^2\alpha^2(\xi R + R_2)}\frac{\partial^2 w}{\partial \xi^2} \quad (22)$$

3. Solution

Finite difference scheme is implemented to solve the equations (17) and (18) along with the boundary conditions (19). The step lengths in the z-direction (Δz,), ξ –direction $\Delta\xi$ and t directions Δt are taken as $z_i = i\Delta z, i = 0,1,\cdots,n$, $\xi_j = j\Delta\xi, j = 0,1,\cdots,J$, $t_k = k\Delta t, k = 0,1,\cdots,K$. If $w_{i,j}^k$ denotes the value of w at (z_i, ξ_j, t_k), then derivatives are replaced with the following forward in time and central in space difference approximations.

$$\left.\begin{aligned}
\frac{\partial w}{\partial \xi} &= \frac{1}{2}\left[\frac{w_{i,j+1}^{k+1} - w_{i,j-1}^{k+1}}{2\triangle\xi} + \frac{w_{i,j+1}^{k} - w_{i,j-1}^{k}}{2\triangle\xi}\right], \\
\frac{\partial^2 w}{\partial \xi^2} &= \frac{1}{2}\left[\frac{w_{i,j+1}^{k+1} - 2w_{i,j}^{k+1} + w_{i,j-1}^{k+1}}{(\triangle\xi)^2} + \frac{w_{i,j+1}^{k} - 2w_{i,j}^{k} + w_{i,j1}^{k}}{(\triangle\xi)^2}\right], \% \\
\frac{\partial w}{\partial t} &= \frac{w_{i,j}^{k+1} - w_{i,j}^{k}}{\triangle t},
\end{aligned}\right\} \tag{23}$$

Similarly $\frac{\partial \nu}{\partial \xi}, \frac{\partial^2 \nu}{\partial \xi^2}, \frac{\partial \theta}{\partial \xi}, \frac{\partial^2 \theta}{\partial \xi^2}, \frac{\partial \nu}{\partial t}$ *and* $\frac{\partial \theta}{\partial t}$ can be defined.

4. Results and discussion:

Flow rate, shear stress and impedance of blood flow in bifurcated artery of Corona patient has been obtained numerically by computational procedure. We used the following data to analyse the various physical quantities with parameters: a = 0.5 cm, d' = 1 cm, l_0 =0. 5 cm, m=10, r_1 =0.51a, τ_m =2a, G_0 = 10N/m^3 and G_1 = 0.2G_0.

Figure 2 explores the results of flow rate over the bifurcated artery of Corona patient near to apex for distinct values of N in appearance of a pulsatile pressure. Volumetric flow rate of Corona patient blood is decreasing with increasing values of N. It is worth to notice that Newtonian fluid gives a higher flow rate than the micropolar fluid model. This is due to microrotation of blood particles and the relative rotational motion between vorticity and microrotation.

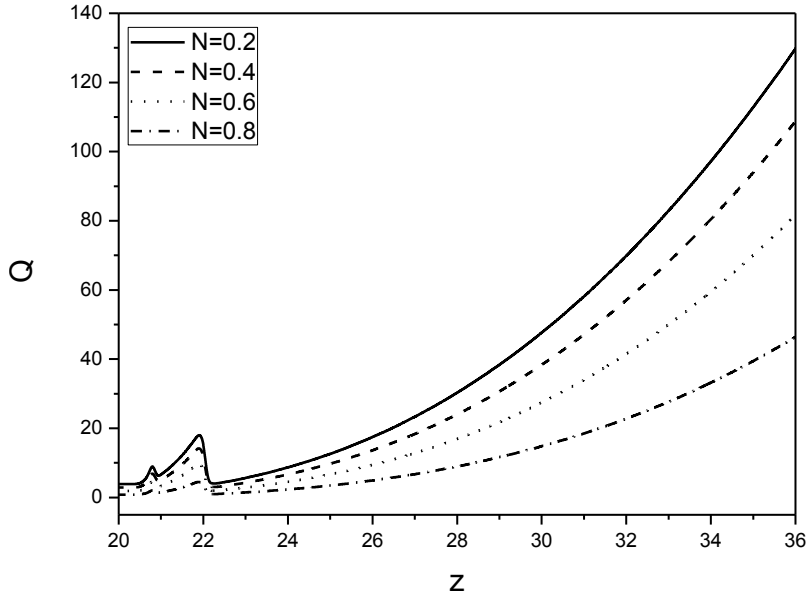

Figure 2: Alterations of volume of flow near flow divider and in daughter artery with N.

Figure 3 includes results for flow rate in the bifurcated artery of Corona patient near to apex with different values of β. It reveals that flow rate is enhancing with an enhancement in values of β in children artery.

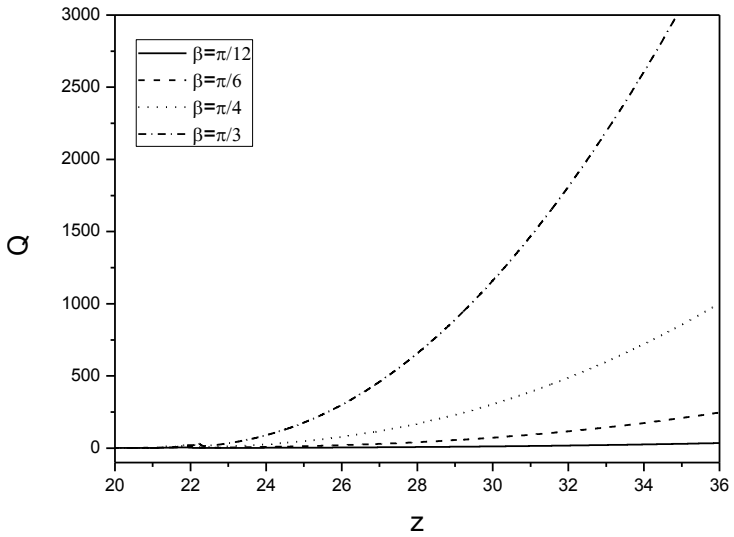

Figure 3: The variation of volumetric flow rate near the apex with β.

Effect of time and the Womersley number on volumetric flow rate patterns of streaming blood of Corona patient along axial direction for two sides of flow division is shown in fig.4. It is seen that volumetric flow rate is enhancing with a better value of time.

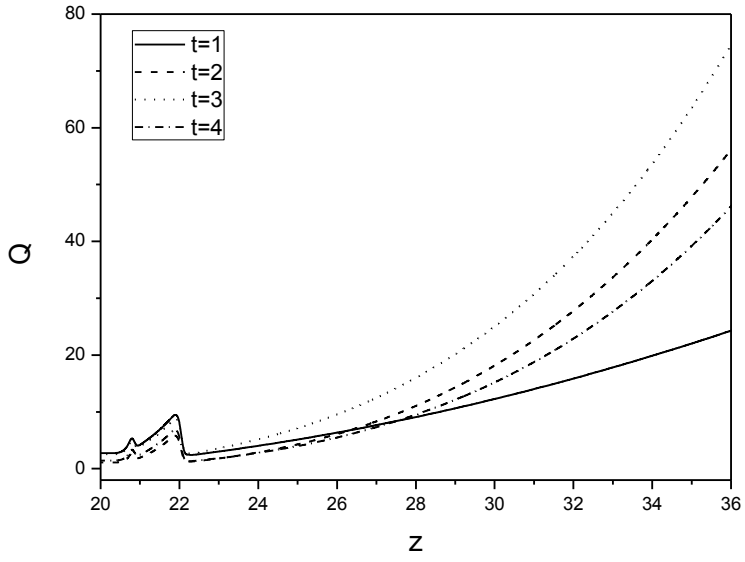

Figure 4: Alteration of volume of flow near the apex with time

The effect of Womersley number on volumetric flow rate patterns of the streaming blood along the axial direction for both sides of the apex is shown in fig.5.

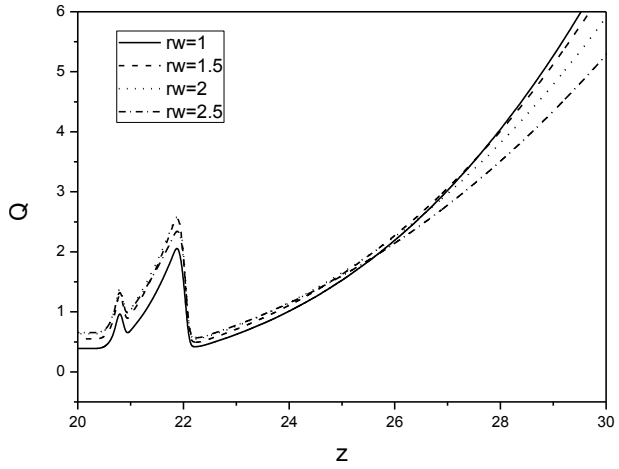

Figure 5: Alteration of volumetric flow rate near the division with R_w

From this fig., it is notices that effect of Rw on flow rate is almost similar to that of time but trend is reversal. It is interesting to notice from the figs.2-5 that the flow rate is disturbed largely adjacent to division of artery. This is because of existence of reverse flow adjacent to the apex. Further, it is recorded that flow rate is locally escalating till inset of lateral junction, a minor deceleration and then rise until the apex. Thereafter flow rate is steadily rising till z_{max}. If a person exposed to corona virus, there is possibility of occurrence of mild stenosis in the arterial system. Due to this, sudden numbness or weakness will be exposed may be leads to paralysis.

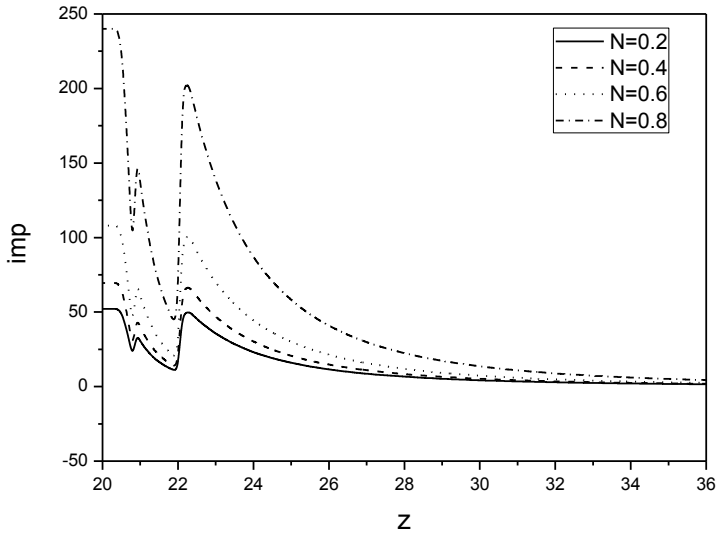

Figure 6: The variation of impedance near the apex with N.

The impact of coupling number on the impedance is presented in fig.6. Impedance is enhancing with an enhancement in value of N. Since $N \to 0$ is related to viscous fluid case, impedance in the case of viscous fluid is fewer than that of micropolar fluid. Hence, the microstructure becomes significant in enhancing the impedance.
The impact of time t on impedance near to apex is revealed in fig7. Impedance is rising with an escalation in time.

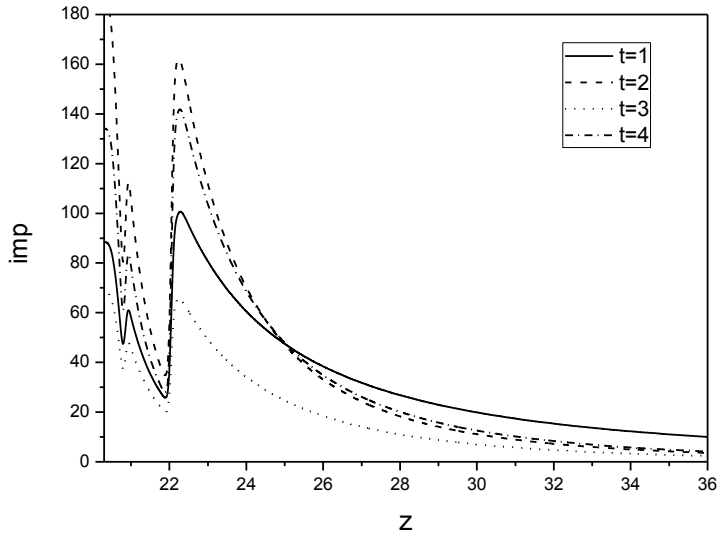

Figure 7: The variation of impedance near the apex with time t.

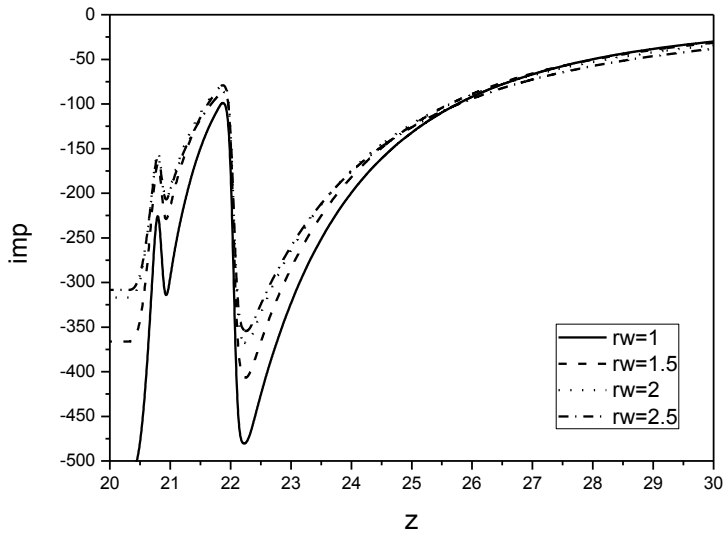

Figure 8: The variation of impedance near the apex with R_w

The impact of Womersly number Rw on the impedance near the apex is revealed in fig.8. Impedance is decreasing with an escalation in Rw. In general, it is found from

figs.6-8 that, as the value of z rises, the impedance is diminishing until inset of lateral junction, slightly increasing within the small range of z, gradually decreasing till the apex and then increasing quickly. Thereafter, it is found that the impedance is uniformly decreasing till z_{max}. The reason behind this behaviour is divergence of blood flow at division of the carotid artery of Corona patient.

Impression of time on the shear stress parallel with walls of child artery is shown in fig.9. From this fig. it is perceived that shear stress at walls inside and outside of the daughter artery is enhancing with a rise in t.

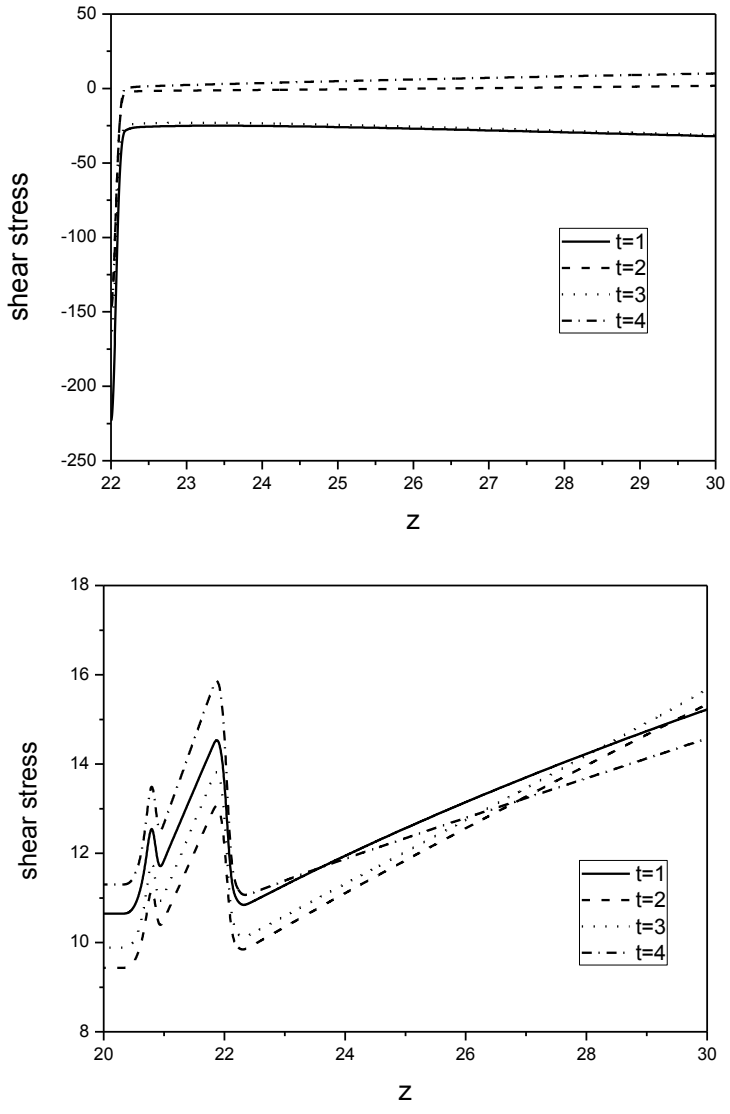

Figure 9: The variation of τ along the wall inside and outside of daughter artery with t

Variation of τ at the daughter artery with coupling number N is demonstrated in fig.10. It is depicted from fig.10 that shear stress along daughter artery is enhancing with an

escalation in the value of N. Further, an enhancement in the values of N decreases shear stress parallel with outer wall of child artery of Corona patient

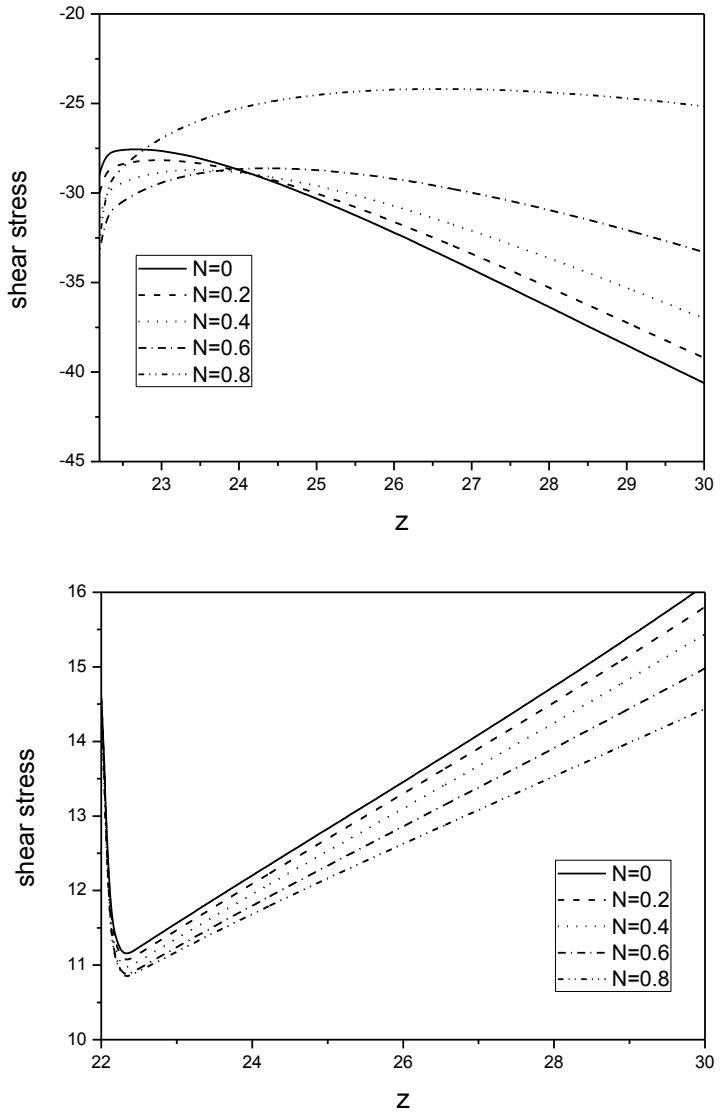

Figure 10: The variation of τ along the wall inside and outside of the daughter artery with N

6. Conclusions

The present investigation analyses the Corona patient's blood flow through bifurcated artery and following are the conclusions

- Shear stress parallel with the outer wall is rising with a rise in values of t, β and reducing with a growth in N. Shear stress along the inner wall is rising with a rise N. The reverse trend is observed for β.

- Flow rate is enhancing with an enhancement in t, Rw, β and diminishing with an increase in N.
- Impedance is rising with a rise in the values of N, t, Rw. Different behaviour is notices at the apex of the carotid artery.

References

[1] Antonova, N. Tosheva, P. and Velcheva, I. (2012), Numerical analysis of blood flow and common carotid artery hemodynamics in the carotid artery bifurcation with stenosis, Series on Biomechanics, Vol. 27, PP. 5-10.

[2] Bose, S. and Banerjee, M. (2015), Magnetic particle capture for biomagnetic fluid flow in stenosed aortic bifurcation considering particle–fluid coupling, Journal of Magnetism and Magnetic Materials, Vol. 385, PP. 32–46.

[3] Bhuvana Vijaya, R, Maruthi Prasad, K. and Umadevi, C. (2016), A mathematical model for micropolar fluid flow through an artery with the effect of stenosis and post stenotic dilatation, Applications and Applied Mathematics: An international Journal, Vol. 11, No. 2, PP. 680-692.

[4] Chakravarty, S. and Senn, S. (2006), A mathematical model of blood flow and convective diffusion processes in constricted bifurcated arteries, Korea-Australia Rheology Journa*l*, Vol. 18, No. 2, PP. 51-65.

[5] Ellahi, R., Rahman, S., Nadeem, S. And Akbar. (2014), Influence of Heat and Mass Transfer on Micropolar Fluid of Blood Flow Through a Tapered Stenosed Arteries with Permeable Walls, Journal of Computational and Theoretical Nanoscience*, Vol.* 11, PP. 1156-1163.

[6] Eringen, A.C.(1966), Theory of micropolar fluids, Journal of Applied Mathematics and Mechanics, Vol. 16, PP. 1–16.

[7] Mekheimer, S. and Kot, A.E. (2008) The micropolar fluid model for blood flow through a tapered artery with a stenosis, Acta Mechanica Sinica, Vol. 24, PP. 637–644.

[8] Sarifuddin, S. Chakravarty, S. and Mandal, P.K. (2013), Heat transfer to micropolar fluid flowing through an irregular arterial constriction, International Journal of Heat and Mass Transfer, Vol. 56, PP. 538–551.

[9] Sapna Ratan Shah, Purnima Chaturvedi, Shabab Akbar and Rohit Kumar, (2021), Prospective of Hydroxychloroquine and Zinc with Azithromycin for Nanoparticles Blood Flow in Covid-19 Patients, International Journal of Nanotechnology in Medicine & Engineering, Vol. 6, No. 1, PP. 1-7.

[10] Shaw, S., Gorla, R.S.R., Murthy, P.V.S.N. and Ng, C.O. (2009), Pulsatile Casson Fluid Flow Through a Stenosed Bifurcated Artery, International Journal of Fluid Mechanics Research, Vol. 36, No. 1, PP. 43-63.

[11] Shit, G.C. and M Roy, M. (2011), Pulsatile flow and heat transfer of a magneto-micropolar fluid through a stenosed artery under the influence of body acceleration, Journal of Mechanics in Medicine and Biology, Vol. 11, PP. 643-661.

[12] Srinivasacharya, D. and Madhava Rao, G. (2016), Magnetic effects on pulsatile flow of micropolar fluid through a bifurcated artery, World Journal of Modelling Simulation, Vol. 12, No. 2, PP. 147-160.

[13] Srinivasacharya, D. and Madhava Rao, G. (2018), Pulsatile Flow of Couple Stress Fluid Through a Bifurcated Artery, Ain Shams Engineering Journal, Vol. 9, PP. 883-893.

[14] Violeta Carvalho, Diana Pinho, Rui A. Lima, José Carlos Teixeira and Senhorinha Teixeira, (2020) Blood Flow Modeling in Coronary Arteries: A Review, fluids, Vol. 6, No. 53, doi.org/10.3390/fluids6020053.

[15] Wu, A., Peng, Y., Huang, B., Ding, X., Wang, X., Niu, P. and Jiang, T. (2020), Genome composition and divergence of the novel coronavirus (2019-nCoV) originating in China, Cell Host & Microbe, Vol. 27, No. 3, PP. 325–328.

[16] Yang, C. and Wang, J. (2020), A mathematical model for the novel coronavirus epidemic in Wuhan, China. Mathematical Biosciences and Engineering, Vol. 17, No. 3, PP. 2708–2724.